

# Image Noise in Dry Powder Electrophotography

John G. Shaw, Dale Mashtare, Paul Morehouse, Michael Thompson, and John Knapp; Xerox Research Center Webster; Webster, New York, 14850

## Abstract

Through both physical experiments and detailed computer simulations, we examine some of the underlying causes of image noise in dry-powder xerography. Although examples are drawn from common electrographic technologies, such as powder-cloud jumping development, our goal is to identify and quantify the limits of toner-based printing systems without regard to any specific product-intent hardware. Understanding and modeling the principle forces between charged toner particles (and surfaces) allows us to simulate complex self-organizing structures that evolve during the development process. It is hoped that studying how these structures form, and how toner properties affect their formation, will lead to improved dry-powder printing technologies that rival lithography.

## Introduction

Using the Xerox Particle Simulation Environment (XPSE) [1] [2], a series of photoreceptor and development simulations were conducted in order to study how photoreceptor thickness, ROS beam size, and toner size fundamentally affects image noise and quality. Rather than emulate any specific imaging and development apparatus; a form of idealized powder-cloud development was simulated where the objective is to create very gentle, but physically realistic, conditions for dry-powder xerography. The underlying premise is that if toner particles are allowed to gently anneal into place on a latent image, they will settle into their minimum-energy configuration. Under such conditions, image noise will be minimized.

A brief overview of XPSE is presented, and some details of the simulation technique discussed. Examples will be shown based on a small, highly detailed, kanji character; imaged with various sizes of toner. Realistic particle size, charge, and adhesion distributions are used by the simulation code. The ultimate goal of these studies is to understand and minimize local image noise in colored halftone images.

## Overview of XPSE

XPSE is a set of C++ libraries and computer programs that are designed to enable the simulation of xerographic subsystems; such as erasure, charging, exposure, development, transfer, and fusing. The underlying code uses the particle-in-cell technique [3] to model individual toner particles in three spatial dimensions and time. Appropriate forces are calculated which describe the effects of collisions with other particles and geometric objects. The software architecture is fully object-orientated and can be thought of as an “operating system for particles”. As the simulation time progresses, *events* (e.g., particle-to-particle collisions) are detected, posted, and subsequently processed by registered *event handlers* (e.g., the force between two colliding particles is computed).

XPSE provides a small three-dimensional CAD-like class library where all geometric objects (e.g., blocks, plates, cylinders, and spheres) are “physically active”. Moving donor and receiver surfaces are available for a number of development subsystem models. Simulations of transfer and fusing are evolving to include detailed air breakdown effects and pressure-driven flow of melted toner layers on paper. Many aspects of toner, carrier bead, and ion particles can be represented, including: stochastic size and charge distributions, inter-particle conduction, magnetic interactions (i.e., for simulating the formation of magnetic brushes), particle-particle cohesion, and particle-boundary adhesion. The particle cohesion and adhesion models support a variety of force components such as: hard-core collisions, complex short-range forces due to charged surface patches and Van der Waals effects, induced electrostatic and magnetic polarization, and friction. Long range electrostatic fields are solved on finite-element grids and blended with shorter-range forces that are calculated within the event-handler functions.

By assembling XPSE components (e.g., finite-element grids, collections of toner particles, geometric objects, numerical field-solvers, etc.), it is possible to create digital simulators that emulate the behavior of specific pieces of hardware. These constructs may be thought of as *virtual fixtures*, and can be used by scientists and engineers to supplement experimentation on conventional *physical fixtures*. XPSE is suitable for problems where the number of cells and particles are on the order of  $10^3$  to  $10^6$ . Run times vary widely with the problem being solved, but can range from minutes to tens of CPU hours on a modern PC/Linux workstation.

It should be noted that XPSE is capable of modeling far more complex xerographic systems than those presented in this short paper. A multilayered photoreceptor model is available that supports a number of virtual imagers (e.g., a conventional or VECSEL laser ROS, and a LED-bar array). Detailed exposure profiles can be computed within the virtual photoreceptor’s charge-generation layer; and the resulting free charge transported to its surface using realistic transport physics. Several variations of field-dependent quantum efficiency and electron-hole mobility models are supported by the underlying simulation codes.

## Limits of Xerography

For purposes of this discussion, “image noise” is considered to be any unwanted component of an image, virtual or real, along any portion of the xerographic image path. This includes all aspects of images on the photoreceptor, intermediate transfer belt or drum, and of course the final sheet of paper. Although Xerox engineers have long applied various modeling techniques to the image path, the present approach uses virtual toner particles to directly simulate the final image on paper. Such simulations have the unique ability to represent *all components* of the final image, including those which manifest themselves for unforeseen reasons. Unlike modeling techniques based on point-spread or modulation-transfer functions, no explicit analytic basis functions are present which can unduly influence the final result. Of course, one needs

to carefully interpret the generated data and be aware of the inherent limitations of the underlying physical models.

### Gentle Powder-Cloud Development

The premise of this work is that the ideal dry-powder image is the one that minimizes the stored potential energy of all toner particles that make up that image, consistent with all relevant boundary conditions. The prevalent boundary conditions include: a) the physical surface of the photoreceptor; b) the latent charge image that exists within the exposed photoreceptor; c) the electrostatic fields in the vicinity of the photoreceptor, including those induced by all external and internal means; and d) the state of the toner particles, including all size, charge, and mechanical effects. For this work, we will consider only the effects of the photoreceptor and development subsystem on image noise. A simple virtual fixture was constructed as illustrated in figure 1.

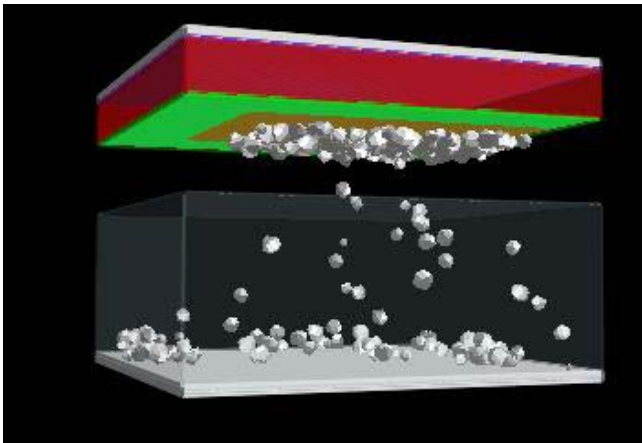


Figure 1: Powder-cloud virtual fixture. The upper surface is the photoreceptor with a rectangular latent image, shown in orange. The lower surface is a metallic plate with a negative DC bias potential. Toner particles are spawned within the lower gap region to maintain a set concentration.

This construct represents a section of a development nip. It is not intended to be part of any specific product, but only a vehicle to study image formation. The upper structure is an imaged photoreceptor, and the lower gray member is a biased metallic plate. This picture shows toner particles migrating from the lower nip region onto the surface of the photoreceptor, which in this case contains the latent charge image of a rectangular halftone dot.

The above surrogate nip maintains a constant concentration of toner in its lower region which is allowed to slowly migrate, under DC bias, towards the latent image. Small random forces are used to “stir” the cloud and keep the toner particles in motion. This approach is a form of simulated annealing, and likely results in the best possible developed image, consistent with the geometry, electrostatic fields, and toner properties.

### Experimental Observations

A series of experiments with a modified xerographic print engine were conducted to study how small toner particles (e.g., 4.0, 5.8, and 7.0 microns) affect image quality. The physical print engine used a conventional two-component magnetic brush to develop latent images on a drum photoreceptor. The photoreceptor was not particularly thin (e.g., 32 microns) and used an over-sampled 800 dpi VECSEL ROS to expose a series of fine kanji

characters (i.e., 3-point fonts with an image area of approximately 1 mm<sup>2</sup>). Figure 2 shows microphotographs of the resulting fused images on paper. It is surprising how well the four-micron toner resolved the fine details of this character. We believe that the thickness of the photoreceptor is ultimately limiting the quality of this character. This observation led to a number of XPSE-based simulations which were used to study the underlying effects of photoreceptor thickness and toner particle size on image quality.

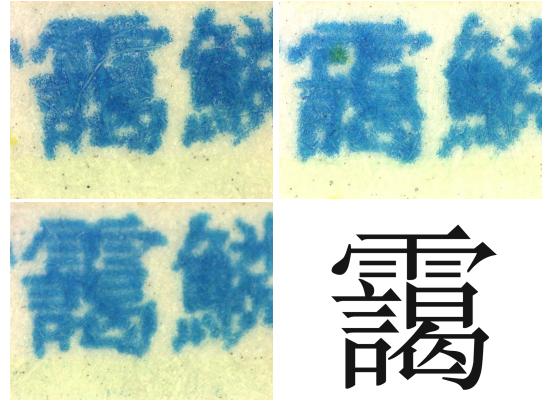


Figure 2: Physical images of three-point kanji character developed and fused to paper with varying toner sizes of 7.0 (upper left), 5.8 (upper right), 4.0 (lower left), microns. The bitmap image pattern is shown in the lower-right quadrant. (Experimental images provided by P. Morehouse)

### Photoreceptor Thickness Study

Figure 3 presents a series of simulated latent images of the kanji character using a virtual 600 dpi ROS. In this case, a four-point font was used rather than a three-point font. The laser’s beam size was set to 38 x 27 microns (FWHM) and no overcoat was present on the virtual photoreceptor. Blue represents background areas with a large negative surface charge, while red indicates where the laser has partially discharged the photoreceptor.

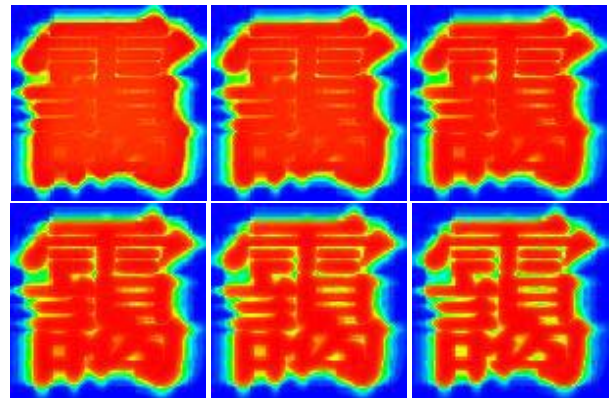


Figure 3: Simulated four-point kanji character's latent image versus varying photoreceptor thickness. Transport thickness from upper left to lower right: 40, 35, 30, 25, 20, and 15 microns. The laser's beam size was set to 38x27 microns.

As might be expected, the latent image improves as the photoreceptor’s transport thickness decreases. This effect is primarily due to reduced charge spreading in thinner photoreceptors. Figure 4 shows a similar series of images, but in

this case the beam size was reduced to 19 x 13.5 microns. Although this narrow beam is not consistent with a 600 dpi laser ROS, this enables us to evaluate the effect of beam width on the latent image, with all other factors held constant. One significant advantage of having a detailed physical simulation capability is to isolate parts of the problem without any unintended side effects. This feature becomes more evident in the following toner size studies where it is very difficult to change only the toner's size without changing anything else, like its charge.

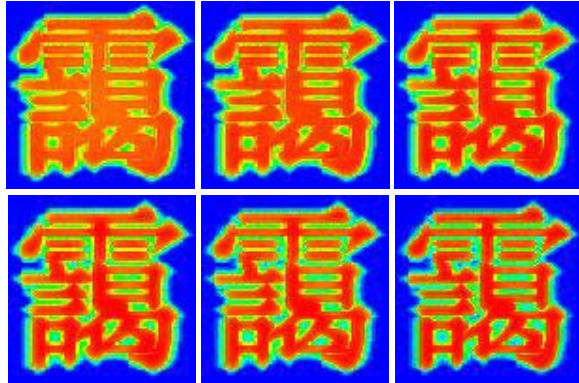


Figure 4: Simulated four-point kanji character's latent image versus varying photoreceptor thickness. Transport thickness from upper left to lower right: 40, 35, 30, 25, 20, and 15 microns. The laser's beam thickness was set to 19x13.5 microns.

### Toner Size Study

Figure 5 contains four simulated images of the same kanji character that was developed with the above virtual fixture using different toner sizes. In all cases, the latent image was defect free (*i.e.*, no ROS was modeled) and resolved to two microns. Similarly, the transfer and fusing stages are essentially perfect, in the sense that they do not introduce any measureable noise into the final image. The imaged area is approximately 1.4 x 1.4 microns. The virtual toner's size distribution is Gaussian, with a standard deviation equal to one-fifth its mean diameter. In all cases, the bulk charge-to-mass ratio was maintained at  $-20 \pm 4 \mu\text{C}/\text{mg}$ . The only parameters varied in the simulations were the mean particle diameter and the volume concentration of toner in the nip region. The latter was adjusted from run-to-run to maintain a constant volume-mass density independent of the particles' size. The images were allowed to develop until an equivalent area-mass density of  $0.5 \text{ mg}/\text{cm}^2$  was obtained. In practice, approximately 90% of the image charge had been neutralized, which is typical for a development subsystem.

Two important observations can be noted. First, the number of particles forming the character increases very rapidly as the particle size is diminished. If a few particles are "out of place", the effect on the final image is low. Second, smaller toner tends to fill in fine structure far better than larger particles do. This is due to the inherently low momentum of the smaller toner. Simulations indicated that all toner moves at approximately the same speed (*e.g.*,  $\sim 1 \text{ m/s}$ ), so the momentum falls as  $r^3$ . Low momentum particles have a much better chance of following the field lines to their optimal position, and also do not perturb nearby particles already on the photoreceptor's surface. In practice this means that

less scavenging leads to better image quality. Contrary to one's first impression, any image quality improvement is not directly due to smaller particles being hard to see. The largest particles are still far too small to be discerned by the naked eye. It's the underlying mass variations that lead to image noise.

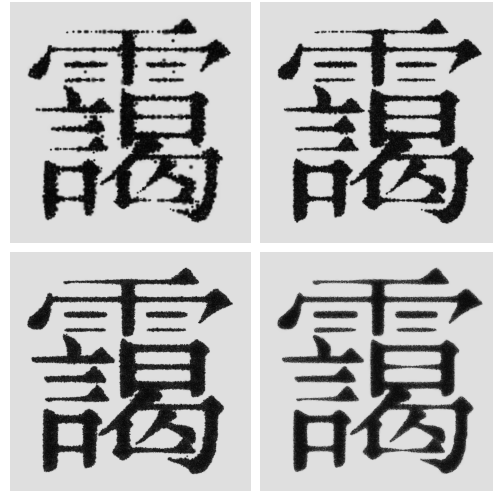


Figure 5: Simulated four-point kanji character developed with varying toner sizes of 10 (upper left), 8 (upper right), 6 (lower left), and 4 (lower right) microns. The particles have realistic size, charge, and adhesion distributions. However, the latent image used by this simulation is essentially perfect.

As mentioned at the end of the previous section, we often use the simulations to isolate one particular aspect of a problem; in this case how particle size affects image quality. This is physically unrealistic, but useful. In a "real" development system, the fixture operator would likely adjust many parameters to achieve an idea setup condition. For example, the images in figure 5 were created using identical charge-to-mass ratios even though the particle diameter varied significantly. Similarly, the DC development bias was held constant, so line shrinkage or growth is not optimal for any of the above images; its just "good enough" for this study.

### Combined Study

In figure 6 we see a series of simulated character images which were generated by combining the latent image simulations with the development simulations. In this case, a three-point character (as used in the physical fixture) is imaged by a simple 600 dpi ROS, and then developed with four different virtual toner packages. As with the images in figure 5, the transfer and fusing stages were very simple models, not physically realistic simulations (*i.e.*, fusing is implemented as a Gaussian blur of the toners' projected mass density).

The resulting images appear even worse than the images generated by the hardware fixture. We believe this is because the hardware ROS was superior to our virtual ROS. Its interesting to note that the binary bitmap image of the kanji character just barely resolves the three-point font at 600 dpi. If one tries to create a bit-mapped two-point font by down sampling the original high-resolution image, all image components merge in to a single blob. Even so, it is clear that small toner results in significantly better fused images.

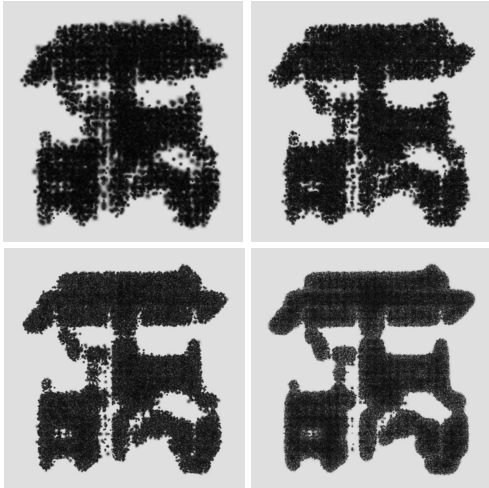


Figure 6: Simulated three-point kanji character developed with varying toner sizes of 10 (upper left), 8 (upper right), 6 (lower left), and 4 (lower right) microns. Unlike in figure 5, the latent image is formed by a simulated 600 dpi ROS with a 32 micron photoreceptor.

### Halftone Dots and Color Stability

So far, this paper has used a single complex kanji character to illustrate the effects of photoreceptor thickness, ROS beam size, and toner size on localized image noise. The main point of this work is to optimize halftone dots in a color xerographic print engine. Exceptional pictorial image quality relies on generating identical dots, each and every time. The best way to achieve this goal is to reduce edge and fill variation (*i.e.*, noise!) by virtual of the underlying physical process and materials package.

Figure 7 shows a 1.8 x 1.8 mm section of a simulated halftone pattern (a large area by XPSE standards!). A 1200 dpi virtual ROS imaged the pattern in a similar manner to that used when imaging the kanji characters in the previous sections of this paper. The beam size was set to 19 x 13.5 microns, hence there is a slight asymmetry in the pattern with respect to the process (across) and beam (down) directions. The individual dot was arranged on an 8 x 8 grid, with the inner square of 16 pixels turned “on” and the outer ring of 48 pixels turned “off”. Thus the true dot shape is that of a perfect square with 25% area coverage.

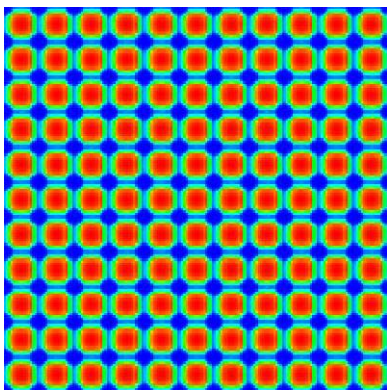


Figure 7: Latent charge image of a simulated halftone dot using a 1200 dpi ROS with a 32 micron photoreceptor. Each dot’s “cell” is 168x168 microns. The laser writes from top to bottom, and the beam is wider in the process direction (*i.e.*, across the page).

Some rounding of the dots’ in the latent image is evident, due to a combination on the laser’s beam shape and charge spreading in the photoreceptor. Finally, the developed halftone image is shown in figure 8. Six-micron toner was used in the development stage. Individual dots generally track the latent image, but even more rounding is present. Isolated toner particles which appear in the clear region between dots are not due to improper setup or over development, as would be expected with “background” particles. They are a result of insufficient resolution of the latent image. Note that each “dot” is actually different from every other dot, which is a source of image noise in half-toned pictures.

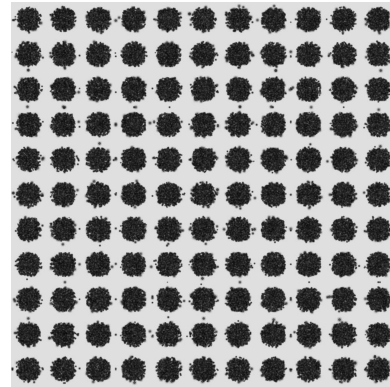


Figure 8: Simulated halftone dot with 6 micron toner. The latent image is that shown in figure 7.

### Conclusions

Though the use of physically-realistic computer simulations, we can gain insight into how common engineering parameters, such as photoreceptor thickness and toner particle size, drives localized image noise in both printed characters and halftone dots. Although equivalent physical experiments can be performed, it is often difficult to control unwanted side effects and isolate the underlying root cause of image noise. In addition, the cost of varying material parameters, in terms of both time and money, can be significantly greater than the cost of these simulations.

### References

- [1] J.G. Shaw and T. Retzlaff, Particle Simulation of Xerographic Development, IS&T Proc., 12<sup>th</sup> Int. Cong. On Digital Printing Technologies, pg. 283-287 (1996).
- [2] J.G. Shaw and T. Retzlaff, Pseudoforce Based Computation of Charged Particle Dynamics. Proc. 20<sup>th</sup> Annual Meeting of the Adhesion Society, pg. 223-225 (1997).
- [3] R.W. Hockney and J.W. Eastwood, Computer Simulation Using Particles (IOP Publishing LTD, 1988).

### Author Biography

John G. Shaw received his PhD in applied physics from the University of Manitoba (1983). Since then he has worked in the Research and Technology Division of Xerox Corporation in Palo Alto, CA, Ithaca, NY (at Cornell University), and Webster, NY. His early career revolved around solid-state physics and amorphous-silicon technology; while his recent work has focused on the development of toner adhesion and transport simulations.